BIOCHEMISTRY
including biophysical chemistry & molecular biology
Article

Biochemistry **2010,** *49,* 2529–2539 2529
DOI: 10.1021/bi9018237

Peroxynitrite-Mediated Oxidative Modifications of Complex II: Relevance in Myocardial Infarction[†]

Liwen Zhang,[‡] Chwen-Lih Chen,[§] Patrick T. Kang,[⊥] Vivek Garg,[∥] Keli Hu,[∥] Kari B. Green-Church,[‡] and Yeong-Renn Chen*[,§,⊥]

[‡]*Campus Chemical Instrument Center, Proteomics and Mass Spectrometry Facility,* [§]*Davis Heart and Lung Research Institute, Division of Cardiovascular Medicine, Department of Internal Medicine, College of Medicine, and* [∥]*Division of Pharmacology, School of Pharmacy, The Ohio State University, Columbus, Ohio 43210, and* [⊥]*Department of Integrative Medical Sciences, Colleges of Medicine and Pharmacy, Northeastern Ohio Universities, Rootstown, Ohio 44272*

Received October 25, 2009; Revised Manuscript Received February 8, 2010

ABSTRACT: Increased $O_2^{\bullet-}$ and NO production is a key mechanism of mitochondrial dysfunction in myocardial ischemia/reperfusion injury. In complex II, oxidative impairment and enhanced tyrosine nitration of the 70 kDa FAD-binding protein occur in the post-ischemic myocardium and are thought to be mediated by peroxynitrite ($OONO^-$) in vivo [Chen, Y.-R., et al. (2008) *J. Biol. Chem. 283*, 27991−28003]. To gain deeper insights into the redox protein thiols involved in $OONO^-$-mediated oxidative post-translational modifications relevant in myocardial infarction, we subjected isolated myocardial complex II to in vitro protein nitration with $OONO^-$. This resulted in site-specific nitration at the 70 kDa polypeptide and impairment of complex II-derived electron transfer activity. Under reducing conditions, the gel band of the 70 kDa polypeptide was subjected to in-gel trypsin/chymotrypsin digestion and then LC−MS/MS analysis. Nitration of Y_{56} and Y_{142} was previously reported. Further analysis revealed that C_{267}, C_{476}, and C_{537} are involved in $OONO^-$-mediated S-sulfonation. To identify the disulfide formation mediated by $OONO^-$, nitrated complex II was alkylated with iodoacetamide. In-gel proteolytic digestion and LC−MS/MS analysis were conducted under nonreducing conditions. The MS/MS data were examined with MassMatrix, indicating that three cysteine pairs, C_{306}−C_{312}, C_{439}−C_{444}, and C_{288}−C_{575}, were involved in $OONO^-$-mediated disulfide formation. Immuno-spin trapping with an anti-DMPO antibody and subsequent MS was used to define oxidative modification with protein radical formation. An $OONO^-$-dependent DMPO adduct was detected, and further LC−MS/MS analysis indicated C_{288} and C_{655} were involved in DMPO binding. These results offered a complete profile of $OONO^-$-mediated oxidative modifications that may be relevant in the disease model of myocardial infarction.

Mitochondrial complex II[1] (EC 1.3.5.1, succinate ubiquinone reductase or SQR) is a key membrane complex in the tricarboxylic acid cycle that catalyzes the oxidation of succinate to fumarate in the mitochondrial matrix. Succinate oxidation is coupled to reduction of ubiquinone in the mitochondrial inner membrane as one part of the electron transport chain. Complex II mediates the transfer of two electrons from succinate to ubiquinone through the prosthetic groups of FAD, [2Fe-2S] (S1), [4Fe-4S] (S2), [3Fe-4S] (S3), and heme *b*. The enzyme is composed of a soluble succinate dehydrogenase hosting a 70 kDa FAD-binding protein, a 27 kDa iron−sulfur protein, and a membrane-anchoring protein fraction hosting two hydrophobic peptides [CybL (14 kDa) and CybS (9 kDa)] with heme *b* binding (*1*).

In the animal disease model of myocardial ischemia and reperfusion injury, oxidative impairment of the electron transfer activity of complex II is marked in the region of myocardial infarction (*2*). The injury of complex II is closely related to the mitochondrial dysfunction (loss of FAD-linked oxygen consumption or state 3 respiration) in the post-ischemic myocardium. Further evaluation of the redox biochemistry of complex II indicated alternations of oxidative post-translational modification are marked in the post-ischemic myocardium, including deglutathiolation (loss of glutathione binding) and an increase in the level of protein tyrosine nitration of the 70 kDa polypeptide of complex II (*2*, *3*).

Myocardial ischemia and reperfusion can provide a stimulus to alter NO metabolism. Enhancement of protein nitration in the myocardium is marked in the post-ischemic heart (*4*−*7*). The marked elevation of the level of protein nitration has been suggested to be due to increased NO production and subsequent superoxide radical anion ($O_2^{\bullet-}$) formation during ischemia and reperfusion (*5*−*7*). This hypothesis has been evaluated in the post-ischemic myocardium of $eNOS^{-/-}$, in which eNOS knockout resulted in a decline in the rate of oxygen consumption by mitochondria and reduction of protein nitration after myocardial

[†]This work was supported by National Institutes of Health Grant HL83237 (Y.-R.C.).

*To whom correspondence should be addressed: Department of Integrative Medical Sciences, Colleges of Medicine and Pharmacy, Northeastern Ohio Universities, 4209 State Route 44, Rootstown, OH 44272. Telephone: (330) 325-6537. Fax: (330) 325-5912. E-mail: ychen1@neoucom.edu.

[1]Abbreviations: complex II, succinate ubiquinone reductase or SQR; $O_2^{\bullet-}$, superoxide anion radical; $OONO^-$, peroxynitrite; DTT, dithiothreitol; ETC, electron transport chain; DCPIP, dichlorophenolindophenol; SMP, submitochondrial particles; SDS−PAGE, sodium dodecyl sulfate−polyacrylamide gel electrophoresis; MS, mass spectrometry; MS/MS, tandem mass spectrometry; β-ME, β-mercaptoethanol; H/RO, hypoxia and reoxygenation; I/R, ischemia and reperfusion.

Published on Web 02/09/2010

infarction (*6*). Therefore, post-ischemic oxygen consumption mediated by eNOS-derived NO is linked to oxidative inactivation of the electron transport chain, including complex II injury. It is well-known that NO traps $O_2^{\bullet-}$ to form peroxynitrite ($OONO^-$) at a very fast rate ($k \sim 10^9-10^{10}$ M^{-1} s^{-1}), thus lending support to the idea that $OONO^-$ formation mediates the enhancement of protein nitration of complex II and other proteins in the post-ischemic myocardium.

In the cellular models of cardiac myoblast H9c2 and endothelium, excess NO can stimulate overproduction of $O_2^{\bullet-}$ in mitochondria via the FAD-binding site of complex II. $OONO^-$-mediated protein tyrosine nitration of the complex II 70 kDa subunit has been reported in posthypoxic H9c2 and fully characterized in the isolated enzyme (*3*). The 70 kDa flavin subunit of complex II contains as many as 18 cysteinyl residues. It is one of the major components to host reactive/regulatory thiols, which are thought to have biological functions such as antioxidant defense and redox signaling. It is logical to hypothesize that other important oxidative post-translational modifications involved in the redox thiols of the 70 kDa subunit can also be mediated by the $OONO^-$ produced during myocardial ischemia and reperfusion. We undertook this study to gain insight into $OONO^-$-mediated oxidative modifications relevant in myocardial infarction. In addition to $OONO^-$-mediated protein tyrosine nitration, we have also detected oxidative modifications of specific cysteinyl residues, including S-sulfonation, disulfide bond formation, and formation of the protein radical intermediate resulting from in vitro $OONO^-$-induced protein tyrosine nitration of complex II.

EXPERIMENTAL PROCEDURES

Isolation of Cardiomyocytes. Adult ventricular myocytes were isolated from Sprague-Dawley rats (~300−350 g) by enzymatic dissociation according to the published procedure by Garg et al. (*8*). Myocytes were placed in 100 mm Petri dishes and incubated at 37 °C in a humidified 5% CO_2/95% air mix prior to the H/RO treatment.

In Vivo Myocardial Regional I/R Model. The procedure for the in vivo I/R rat model was performed using the technique reported in a previous publication (*2*). Sprague-Dawley rats (~300−350 g) were anesthetized with Nembutal administered intraperitoneally (80−100 mg/kg). The left anterior descending coronary artery (LAD) was then occluded. After ischemia for 30 min, the suture around the coronary artery was untied, allowing reperfusion to occur. At 24 h post-infarction, rats were then sacrificed, and the hearts were excised and placed in PBS buffer. The infarct area (or risk region) was delineated by 2,3,5-triphenyltetrazolium chloride (TTC) staining.

Preparations of Mitochondrial Complex II. Complex II was isolated from succinate cytochrome *c* reductase (a supercomplex hosting complex II and complex III) by calcium phosphate-cellulose chromatography under nonreducing conditions according to the published method developed by Yu et al. (*9*, *10*). Succinate was included in all buffers used in the purification procedure. Complex II-containing fractions obtained from the second calcium phosphate-cellulose column were concentrated by 43% ammonium sulfate saturation and centrifugation at 48000*g* for 20 min (*9*). The precipitate obtained was dissolved in 50 mM Na/K phosphate (pH 7.8) containing 0.2% sodium cholate and 10% glycerol. The specific activity of purified complex II is ~15.2 μmol of succinate oxidized or dichlorophenolindophenol (DCPIP) reduced min^{-1} (mg of protein)$^{-1}$.

Analytical Methods. Optical spectra were recorded on a Shimadzu 2401 UV−vis recording spectrophotometer. The protein concentration of complex II was determined by the Lowry method using BSA as the standard. The enzyme activity of complex II was assayed by measuring Q_2-stimulated DCPIP reduction by succinate as described in the literature (*9*). To measure the electron transfer activity of complex II, an appropriate amount of complex II or myocardial tissue homogenate was added to an assay mixture (1.00 mL) containing 50 mM phosphate buffer (pH 7.4), 0.1 mM EDTA, 75 μM DCPIP, 50 μM Q_2, and 20 mM succinate as developed by Hatefi et al. (*11*). The complex II activity was determined by measuring the decrease in absorbance at 600 nm and confirmed by inhibition using thenoyl trifluoroacetone (TTFA). The specific activity of complex II [nanomoles of DCPIP reduced (or succinate oxidized) per minute per milligram of complex II] was calculated using a molar extinction coefficient (ε_{600}) of 21 mM^{-1} cm^{-1}.

Alkylation of Complex II with Iodoacetamide. The sample of nitrated complex II was subjected to alkylation with iodoacetamide (ICH_2CONH_2) to block free thiols on the surface of the protein. Nitrated complex II (0.2 mg/mL) in the reaction mixture was incubated with iodoacetamide (2 mM) at room temperature. After incubation for 1 h, more iodoacetamide was added to a final concentration of 4 mM and the mixture was incubated at 4 °C for 8 h. The gel band of the 70 kDa subunit in the SDS−PAGE gel with nitrated complex II was subjected to in-gel digestion with trypsin, chymotrypsin, or both, which was followed by LC−MS/MS analysis.

In-Gel Digestion and Capillary Liquid Chromatography−Nanospray Tandem Mass Spectrometry (Nano-LC−MS/MS) Analysis. The protein separated by SDS−PAGE gels was digested with sequencing grade trypsin (Promega, Madison, WI), chymotrypsin (Roche, Indianapolis, IN), and a combination of both enzymes following the protocol described in previous studies (*12*). The peptides were extracted from the polyacrylamide with 50% acetonitrile and 5% formic acid several times and concentrated in a speed vac to ~25 μL for LC−MS/MS analysis. Nano-LC−MS/MS was performed on a Thermo Finnigan LTQ mass spectrometer equipped with a nanospray source operated in positive ion mode. The LC system was an UltiMate Plus HPLC system from LC-Packings, a Dionex Co. (Sunnyvale, CA). The sample was first cleaned on the trapping column (LC-Packings) with 50 mM acetic acid before being eluted off onto the column (ProteoPep II C18, 5 cm × 75 μm, New Objective, Inc., Woburn, MA) connected directly in the nanospray tip. Solvent A was water containing 50 mM acetic acid, and solvent B was acetonitrile. Peptides were eluted directly off the column into the LTQ system using a gradient of 2 to 80% B over 30 min with a flow rate of 300 nL/min. The MS/MS data were acquired on the basis of the TopTen method; the analysis was programmed for a full scan recorded between 350 and 2000 Da, and an MS/MS scan to generate product ion spectra in consecutive instrument scans of the 10 most abundant peaks in the spectrum. The CID fragmentation energy was set to 35%. To exclude multiple MS/MS scans, dynamic exclusion is enabled with a repeat count of 30 s, an exclusion duration of 350 s, a low-mass width of 0.5 Da, and a high-mass width of 1.50 Da.

Sequence information from the MS/MS data was processed using the MASCOT 2.0 active perl script with standard data processing parameters to form a peaklist (mgf file). Database

searching was performed against the SWISSPROT database using MASCOT 2.0 (Matrix Science, Boston, MA) for protein identification. The data were also searched with MassMatrix (*13*), for the identification of post-translational modifications (S-sulfonation, tyrosine nitration, and DMPO adducts) and disulfide bond linkage on the 70 kDa subunit. The mass accuracy of the precursor ions was set to 1.8 Da to accommodate accidental selection of the C13 ion, and the fragment mass accuracy was set to 0.8 Da. Possible hits were manually verified.

RESULTS AND DISCUSSION

Peroxynitrite Formation in the Mitochondria of Post-hypoxic Myocytes. Formation of $OONO^-$ in the rat myocardium during I/R injury has been reported (*7*). The marker of $OONO^-$ detected in tissues or cells has been recognized as an indicator that NO and $O_2^{\bullet -}$ are overproduced, subsequently forming $OONO^-$ under the conditions of disease. In a recent study, Han et al. have reported nitrotyrosine staining in the mitochondria of endothelial cells under I/R conditions (*14*). We have conducted a similar experiment using adult rat ventricular myocytes obtained by enzymatic dissociation according to published procedures (*8*). Myocytes were subjected to the control or hypoxia (1 h) and reoxygenation (2 h) (H/RO) at 37 °C prior to immunofluorescence staining. To determine the effects of H/RO-mediated protein nitration, nitrotyrosine in myocytes was examined by immunofluorescence confocal microscopy. A basal level of nitrotyrosine staining was observed in myocytes under the control conditions. A small amount of nitrotyrosine was colocalized with the mitochondrial marker Mitotracker (Figure 1, top panel). Exposing myocytes to hypoxia followed by reoxygenation resulted in substantially more intense nitrotyrosine staining that showed significant localization of nitrotyrosine in mitochondria (Figure 1, bottom panel). The ratio of signal intensity obtained from anti-3-nitrotyrosine antibody to that of Mitotracker Red staining is ~0.49 for the control myocyte and ~0.74 for the posthypoxic myocyte. The merged images showed a significant increase in colocalization between mitochondria and nitrotyrosine staining in the H/RO group (Figure 1, bottom panel). The percentage of colocalization between nitrotyrosine and mitochondria increased from 16% in control group to 34% in H/RO group. A total of 25 cells were analyzed. These results indicate that there is an overproduction of NO and $OONO^-$ formation in mitochondria during I/R injury.

Protein Tyrosine Nitration of the 70 kDa Subunit of Complex II in Myocardial Tissue after Myocardial Infarction. Protein nitration of the complex II 70 kDa FAD-binding polypeptide was evaluated in the disease model of myocardial infarction resulting from I/R injury. Rats were subjected to 30 min of coronary ligation followed by a 24 h reperfusion according to a previously published procedure (*2*, *3*). Tissue homogenates were prepared from the non-ischemic region and infarct region according to a published method (*2*). The electron transfer activity of complex II in myocardial tissue homogenates was measured by Q_2-stimulated DCPIP reduction by succinate as described in Experimental Procedures. As indicated in Figure 2A, complex II activity in the tissue homogenates of the infarction area was decreased by 46.5 ± 8.4% ($n = 6$; $p < 0.01$) compared to that of the non-ischemic area. The immobilized polyclonal antibodies against the 70 kDa fragment were subsequently used to immunoprecipitate the 70 kDa FAD-binding subunit from the

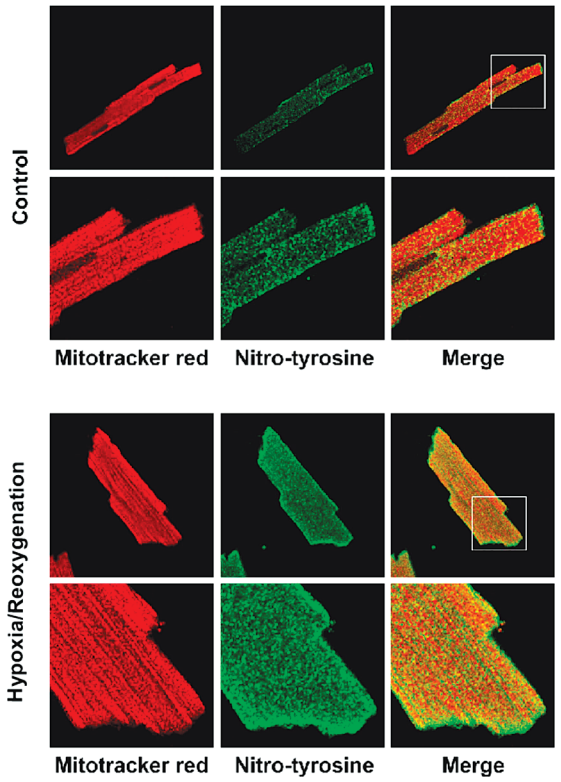

FIGURE 1: Hypoxia and reoxygenation (H/RO) increase the level of 3-nitrotyrosine staining in the mitochondria of myocytes. Cardiomyocytes were plated on laminin-coated coverslips in 24-well plates. Hypoxic treatment was accomplished via formation of a layer of oil on the surface of the glucose-free medium and incubation for 1 h, after which reoxygenation was conducted via incubation in medium with glucose for 2 h. After treatment, myocytes were loaded with Mitotracker Red (250 nM for 15 min), fixed, and stained for nitrotyrosine using an anti-nitrotyrosine polyclonal antibody (the secondary antibody was Alexa 488-conjugated). Fluorescence images were acquired with confocal microscopy and were merged to determine whether the increase in the magnitude of the nitrotyrosine signal colocalized in mitochondria.

tissue homogenate of post-ischemic myocardium, which was followed by immunoblotting with a polyclonal antibody against 3-nitrotyrosine. As indicated in Figure 2B, we have detected a weak signal of nitrotyrosine on the 70 kDa subunit of complex II from the non-ischemic region (Figure 2B, top panel, lane 2). The signal intensity of protein nitration on the 70 kDa subunit of complex II was enhanced in the infarct region of the post-ischemic myocardium (top panel, lane 1). The detected Western blot was abolished by pretreatment of the sample with dithionite due to reduction of 3-nitrotyrosine to 3-aminotyrosine (Figure 2B, top panel, lane 3). The tissue homogenates were further immunoblotted with anti-70 kDa Ab to quantitate the protein loading of SDS−PAGE (Figure 2B, bottom panel). The ratio of signal intensity obtained from anti-3-nitrotyrosine Ab to that of anti-70 kDa Ab is ~1.21 for the infarct region and ~0.32 for the non-ischemic region.

Peroxynitrite-Mediated Protein Tyrosine Nitration of the 70 kDa Subunit of Isolated Complex II. It is widely accepted that protein nitration is the fingerprint of $OONO^-$ overproduction in vivo, and that protein nitration detected in the post-ischemic myocardium is mediated by $OONO^-$. In vitro studies using isolated complex II have the advantage of providing precise measurements and unequivocal results, which can complement the in vivo studies using post-ischemic myocadium. Isolated complex II (1 μM based on heme *b*) was subjected to

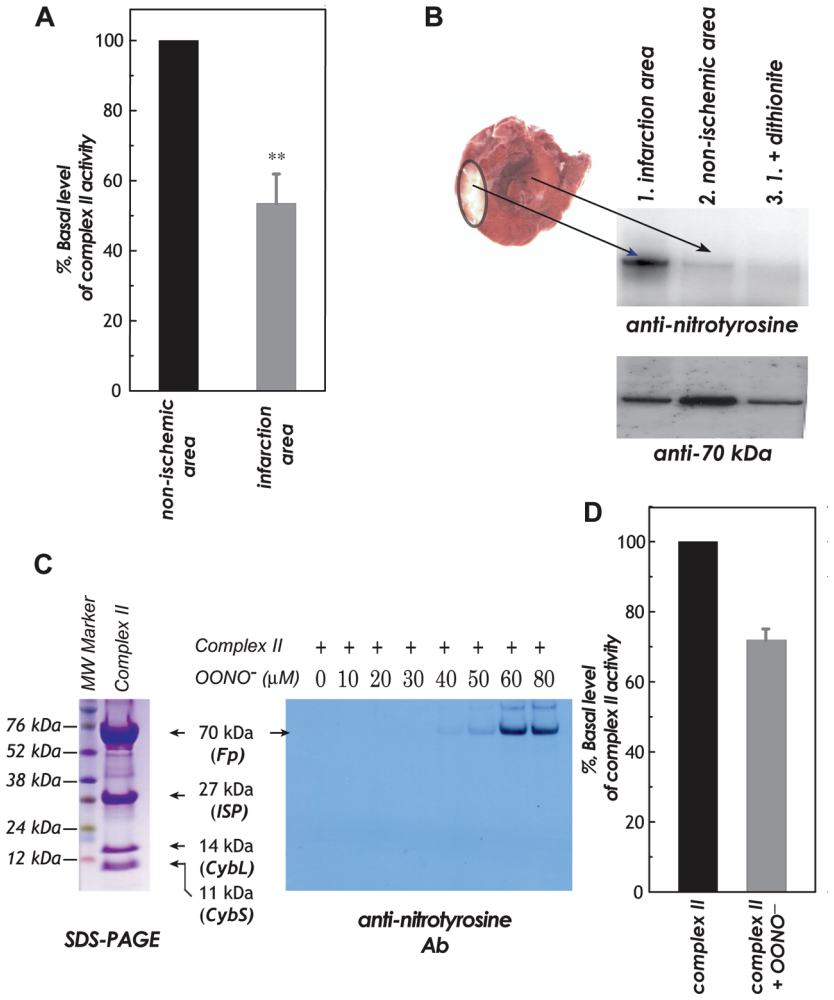

FIGURE 2: (A and B) Rat heart model of in vivo myocardial I/R and TCC staining of the infarct region in the post-ischemic myocardium. Myocardial tissue homogenates from non-ischemic and infarct (risk) regions were subjected to analysis of complex II activity (in panel A) and immunoprecipitation with a polyclonal antibody against complex II 70 kDa and subsequently subjected to SDS−PAGE and immunoblotted with anti-3-nitrotyrosine (top panel) and anti-70 kDa (bottom panel) antibodies (in panel B). Note that 100% of the basal level of enzymatic activity (TTFA sensitive) is 60.3 nmol of DCPIP reduced min^{-1} (mg of protein)$^{-1}$ in panel A. (C) In the right panel, isolated complex II was subjected to in vitro protein tyrosine nitration. Protein (1 μM, based on heme *b*) was incubated with various concentrations of $OONO^-$ (0−80 μM) at 37 °C for 1 h. Excess $OONO^-$ was removed with uric acid (1 mM). $OONO^-$-treated complex II was subjected to SDS−PAGE and then immunoblotting with the anti-3-nitrotyrosine antibody. The left panel shows SDS−PAGE of $OONO^-$-treated complex II stained with Coomassie blue. (D) $OONO^-$-treated complex II was subjected to analysis of electron transfer activity; 100% of the basal level of purified bovine complex II activity is 15.0 μmol of succinate oxidized min^{-1} (mg of protein)$^{-1}$.

in vitro protein nitration using various concentrations of $OONO^-$ (0−80 μM) (*3*). The resulting $OONO^-$-treated complex II was subjected to SDS−PAGE in the presence of β-mercaptoethanol (β-ME) (Figure 2C), which was followed by immunoblotting with anti-3-nitrotyrosine Ab. We observed the 70 kDa subunit of complex II was involved in site-specific protein nitration as indicated in Figure 2C (right panel). The magnitude of the detected Western blot signal was increased in proportion to the dosage of $OONO^-$ used, and the optimal signal intensity of protein nitration was observed at 60 μM $OONO^-$. The electron transfer activity of complex II was decreased by 28.1 ± 1.9%, resulting from $OONO^-$ treatment (Figure 2D, 60 μM $OONO^-$ used, 37 °C for 1 h).

Peroxynitrite-Mediated Cysteine S-Sulfonation of the Complex II 70 kDa Subunit. To gain insight into the complex II-derived oxidative modifications mediated by $OONO^-$, we subjected the protein band of the 70 kDa subunit of $OONO^-$-treated complex II [lane 2 in the SDS−PAGE gel of Figure 2C (left panel) and complex II treated with 60 μM $OONO^-$] to in-gel digestion with trypsin and chymotrypsin and analyzed by LC−MS/MS. With this technique, 93.4% of the amino acid sequence was identified in the MS/MS spectra. The coverage of the amino acid sequence of the complex II 70 kDa subunit is indicated in Figure 3A.

The MS/MS spectra of nitrated complex II were examined for S-sulfonation (conversion of -SH to $-SO_3H$) which occurs during cysteine oxidation. The mass spectra were examined for the mass shift of 48 Da caused by S-sulfonation. Detailed MS/MS analysis provided additional sequential information for the localization of S-sulfonation. For example, a mass shift of 48 Da was seen for the doubly charged ion at m/z 1121.56^{2+} (M + H = 2242.12), compared with that of the unmodified tryptic peptide $_{263}$TYFSC^{267}-TSAHTSTGDGTAMVTR$_{283}$ (theoretical M + H = 2193.9539). Analysis of the MS/MS spectrum of this peptide also revealed that a mass shift of 48 Da was observed in the fragment ions of b5, b6, b9−b14, b16−b19, and y17−y20 (Figure 4), indicating the location of S-sulfonation was C_{267}. Likewise, a mass shift of 48 Da was detected in the MS/MS spectra of doubly charged ions of tryptic peptides $_{467}$AC$_{(CAM)}$^{468}ALSIAESC^{476}RPGDK$_{481}$ (CAM is carbamidomethylation) and $_{529}$VGSVLQEGC^{537}-EKISSLYGDLR$_{548}$ [m/z 813.35^{2+} and 1101.67^{2+} (Figures S1

FIGURE 3: Amino acid sequence of the precursor of the complex II 70 kDa FAD-binding subunit. The regions labeled in bold represent the amino acid residues identified with LC−MS/MS under the reduced conditions in the presence of β-ME (A) and nonreduced conditions in the absence of β-ME (B). In panel A, the cysteinyl residues involved in S-sulfonation are highlighted in gray and they are C_{267}, C_{476}, and C_{537}. The cysteinyl residues involved in protein radical formation are underlined and they are C_{288} and C_{655}. In panel B, the cysteinyl residues involved in the disulfide linkage are highlighted in gray and they are C_{306}, C_{312}, C_{439}, C_{444}, C_{288}, and C_{575}. The region labeled with a dotted underline is the N-terminal extension (amino acids 1−43), which acts as an import sequence and does not exist in the mature protein.

and S2 of the Supporting Information and Table 1)]. Detailed MS/MS analysis provided additional information about the sequences of the two peptides and revealed S-sulfonation occurred at C_{476} and C_{537}, respectively.

On the basis of the X-ray structure of mammalian complex II (Protein Data Bank entry 1ZOY) (*15*), C_{267}, C_{476}, and C_{537} are surface-exposed and therefore are possibly involved in $OONO^-$-mediated S-sulfonation. C_{267} (C_{224} in the mature protein) is located in the hydrophilic pocket of the β-barrel subdomain of the large FAD binding domain. C_{476} (C_{433} in the mature protein) is situated at the terminus of the α-helix in the FAD-binding domain. C_{537} (C_{494} in the mature protein) is located on the surface of the three-helix bundle from the helical domain. All of them are surface-exposed (Figure S3A of the Supporting Information) and, thus, logically susceptible to $OONO^-$-mediated oxidation. Furthermore, all three of these cysteine residues are conserved in the mammalian enzyme, but not in the bacterial enzyme. Therefore, we suggest that these reactive cysteines of mammalian complex II play the regulatory function in response to oxidant stress under the pathophysiological conditions, forming oxidized cysteines.

C_{267} is located in the FAD-binding domain (residues 10−273 in the mature protein). The X-ray structure also reveals that C_{267} is near the riboflavin moiety of FAD (9.0 Å). Sulfonation of C_{267} likely induced a functional impact on the FAD, which subsequently impaired the electron transfer activity of complex II and mitochondrial function in vivo. Sulfonation of C_{476} and C_{537} was not likely to exert a significant impact on the electron transfer activity of complex II due to the much longer distances (23 and 28 Å) from the FAD moiety.

Previous study indicated that superoxide generation is mediated by complex II in the presence of succinate (*2*). Oxidative attack of superoxide-induced protein thiyl radical formation was detected by immuno-spin trapping (*2*). However, cysteine oxidation with S-sulfonation at C_{476} was also detected by LC−MS/MS (m/z 813.42^{2+}, spectrum not shown) under the conditions of superoxide generation by complex II. Therefore, C_{476} is the unique thiol susceptible to S-sulfonation induced by the attack of oxygen free radical(s).

C_{537} has been reported to be the secondary site (C_{90} is the primary site) involved in S-glutathionylation induced by GSH/GSSG in vitro (*2*). Loss of glutathione binding or deglutathionylation has been detected at the 70 kDa subunit of complex II under the conditions of myocardial ischemia and reperfusion (*2*). Presumably, highly reductive conditions of ischemia trigger deglutathionylation of complex II. The detection of S-sulfonation at C_{537} suggests the possibility that S-sulfonation follows deglutathionylation at the same cysteine residue of the complex II 70 kDa subunit under the conditions of ischemia (eq 1) and reperfusion (eq 2).

$$Cys_{537}\text{-S-SG} \rightarrow Cys_{537}\text{-SH} \quad (1)$$

$$Cys_{537}\text{-SH} \xrightarrow{OONO^-} Cys_{537}\text{-}SO_3^- \quad (2)$$

Peroxynitrite-Mediated Cysteine Disulfide Formation of the Complex II 70 kDa FAD-Binding Subunit. Oxidative post-translational modification with disulfide formation in the complex II 70 kDa subunit can occur under conditions of oxidative stress induced by $OONO^-$. To test this hypothesis, iodoacetamide was added to nitrated complex II to block free cysteines through carbamidomethylation (addition of $-CH_2CONH_2$) reaction and thus prevented random disulfide bond formation. Alkylated and nitrated complex II was then subjected to SDS−PAGE under nonreducing conditions in the absence of β-ME. The protein band corresponding to the 70 kDa subunit was subjected to in-gel proteolytic digestion and nano-LC−MS/MS analysis; 86.6% of the amino acid sequence was identified in the MS/MS spectra of the tryptic/chymotryptic peptides of the complex II 70 kDa subunit (Figure 3B). We examined the MS/MS data with MassMatrix (*13*) to identify disulfide bonds formed in this subunit. Possible hits were manually checked, and three cysteine pairs, C_{306}−C_{312} [m/z 802.65^{2+} (Figure 5)], C_{439}−C_{444} [m/z 941.43^{3+} (Figure S4 of the Supporting Information)], and C_{288}−C_{575} [m/z 860.36^{2+} (Figure 6)], were verified as $OONO^-$-mediated disulfide formation (as summarized in Table 1). Disulfide bond formation in protein can be classified as an interchain (disulfide bonds formed between two separate peptides) or intrachain (disulfide bond formed within the same peptide) linkage. Fragmentation of an intrachain linkage generates b and y ions before disulfide bond linkage and corresponding y-2 and b-2 ions after disulfide bond linkage. For example, as shown in Figure 5, the doubly charged peptide at m/z 802.42^{2+} was identified as peptide $_{303}$GAGC^{306}LITEGC^{312}-RGEGGIL$_{319}$ with a disulfide bond between C_{306} and C_{312}. The observed M + H (1603.83) was 2 Da less than the theoretical M + H (1605.7723) of the peptide without a disulfide bond linkage. Fragmentation ions observed in the MS/MS spectrum were y2−y7 and y14-2 (y14*), y15-2 (y15*), and b10-2 (b10*) to b16-2 (b16*), where the loss of 2 Da was caused by the formation of a disulfide bond. These observations, especially the characteristic y-2 and b-2 fragmentation ions, confirmed the linkage between C_{306} and C_{312}. Likewise, fragmentation of an intrachain linkage to generate y-2 and b-2 ions was also detected at the triply charged peptide with

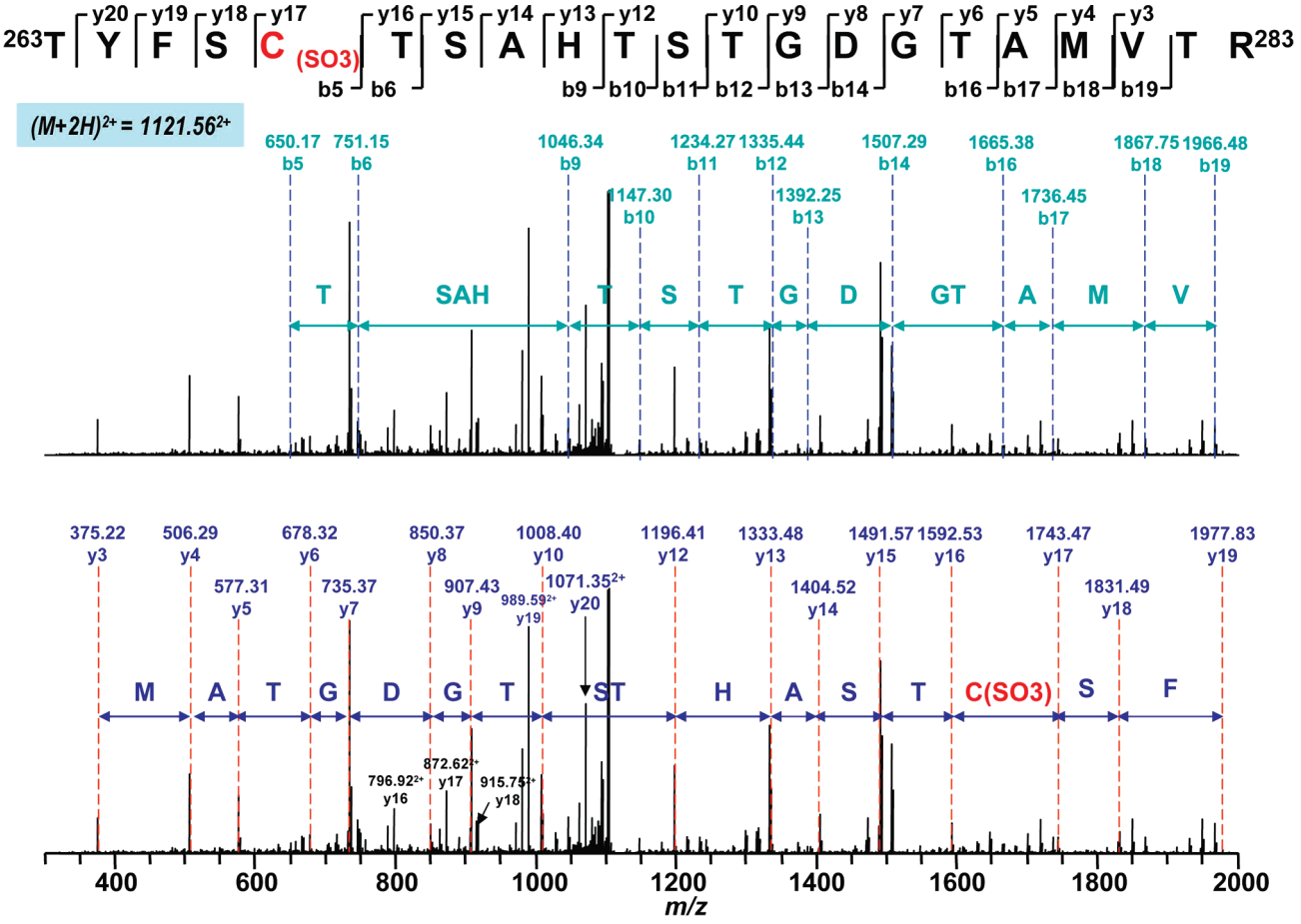

FIGURE 4: MS/MS of the doubly protonated molecular ion of the S-sulfonated peptide [^{263}TYFSC^{267} $_{(SO3)}$ TSAHTSTGDGTAMVTR^{283}] (in which C_{267} was sulfonated) of the 70 kDa subunit from peroxynitrite-treated complex II. The sequence-specific ions are labeled as y and b ions on the spectrum. Note that the same spectrum is shown the top and bottom panels.

Table 1: Summary of the Peptide Sequences and Corresponding Oxidative Post-Translational Modifications (OPTM) Obtained from MS/MS Analysis

amnio acid residue in the 70 kDa fragment	theoretical m/z	observed m/z	peptide sequence and OPTM	remarks
Y_{56}	982.1527^{3+}	982.90^{3+}	^{48}VSDAISAQ**Y$_{56(NO2)}$**PVVDHEFDAVVVGAGGAGLR^{76}	from ref 3
Y_{142}	1286.9052^{3+}	1286.76^{3+}	^{130}GSDWLGDQDAIHYMTEQAPASVVELEN**Y$_{142(NO2)}$**GMPFSR^{163}	from ref 3
C_{267}	1121.4730^{2+}	1121.56^{2+}	^{263}TYFS**C$_{267(SO3)}$**TSAHTSTGDGTAMVTR^{283}	
C_{476}	813.3665^{2+}	813.35^{2+}	^{467}A**C$_{(CAM)}$**ALSIAESC**$_{476(SO3)}$**RPGDK^{481}	$O_2^{\bullet-}$-mediated S-sulfonation
C_{537}	1101.0414^{2+}	1101.67^{2+}	^{529}VGSVLQEG**C$_{537(SO3)}$**EKISSLYGDLR^{548}	glutathionylation (*2*)
C_{306}/C_{312}	802.3820^{2+}	802.42^{2+}	^{303}GAG**C$_{306(SS)}$**LITEG **C$_{312(SS)}$**RGEGGIL^{319}	
C_{439}/C_{444}	941.1017^{3+}	941.43^{3+}	^{425}HVNGQDQVVPGLYA**C$_{439(SS)}$**GEAA**C$_{444(SS)}$**ASVHGANR^{452}	
C_{288}/C_{575}	860.4094^{2+}	860.36^{2+}	^{287}P**C$_{288(SS)}$**QDL^{291}/^{568}ELQNLML**C$_{575(SS)}$**AL^{577}	
C_{288}	789.3871^{2+}	789.85^{2+}	^{284} AGLP**C$_{288(DMPO)}$**QDL EFVQF^{296}	
C_{655}	856.4378^{2+}	856.48^{2+}	^{649} TLN ETD**C$_{655(DMPO)}$**ATVPPA IR^{663}	glutathionylation (*2*)

an m/z 941.43^{3+}, confirming the linkage between C_{439} and C_{444} (Figure S4 of the Supporting Information).

When two cysteine residues were linked through an interchain linkage, each peptide chain may undergo fragmentation independently. Therefore, when one chain is fragmentized to create product ions, the other chain can be considered as a modification to the cysteine residue on the first chain. As shown in Figure 6, the doubly charged peak at m/z 860.36^{2+} was identified as two cysteine-containing peptides, $_{568}$ELANLMLC^{575}AL$_{577}$, and $_{287}$PC^{288}QDL$_{291}$, linked through C_{575} and C_{288}. Fragmentation ions b2A−b7A from chain A and y3B from chain B were observed. Additional sequential information, including M-L, M-AL, M-ELQN, and M-ELQNLML (M represents chain A and chain B), was assigned as b9A, b8A, y6A, and y3A, respectively, if chain B was considered a modification group to C_{575}, while *M*-DL was assigned as b3B if chain A is considered a modification group to C_{288}. Further experiments showed these disulfide bonds containing peptide ions subsequently disappeared under the reducing conditions in the presence of β-ME. In addition, these ions were not observed in the control experiment in which complex II was subjected to iodoacetamide alkylation without $OONO^-$ treatment. LC−MS/MS analysis revealed that C_{306}, C_{312}, C_{439}, C_{444}, C_{288}, and C_{575} were carbamidomethylated as indicated in Table 2. Therefore, these three disulfide bond linkages were formed specifically during the nitration of complex II.

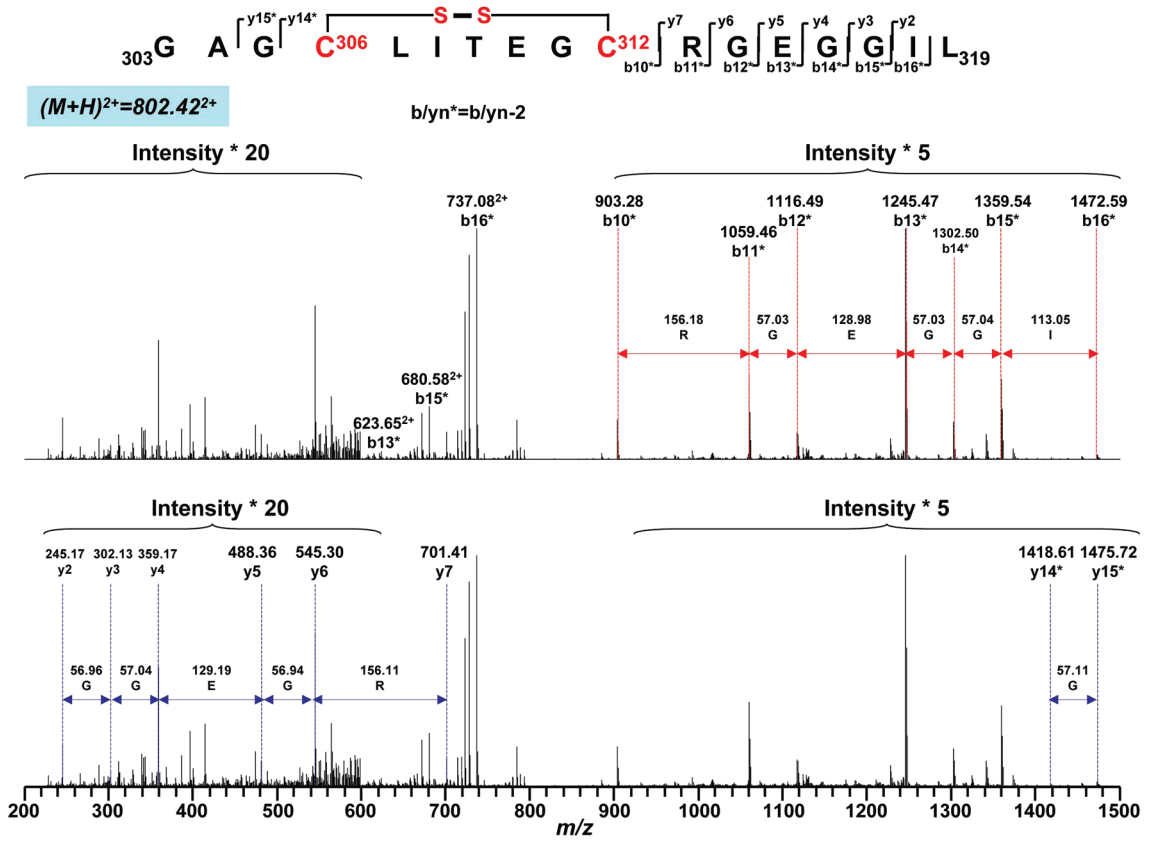

FIGURE 5: Disulfide bond linkage between C_{306} and C_{312} as determined from the MS/MS spectrum of tryptic/chymotryptic digests of the 70 kDa subunit of peroxynitrite-treated complex II. The sequence-specific ions are labeled as y*n* (*n* = 2−7), y*n** (y*n*-2, *n* = 14 or 15), and b*n** (b*n*-2, *n* = 10−16). Note that the same spectrum is shown in the top and bottom panels.

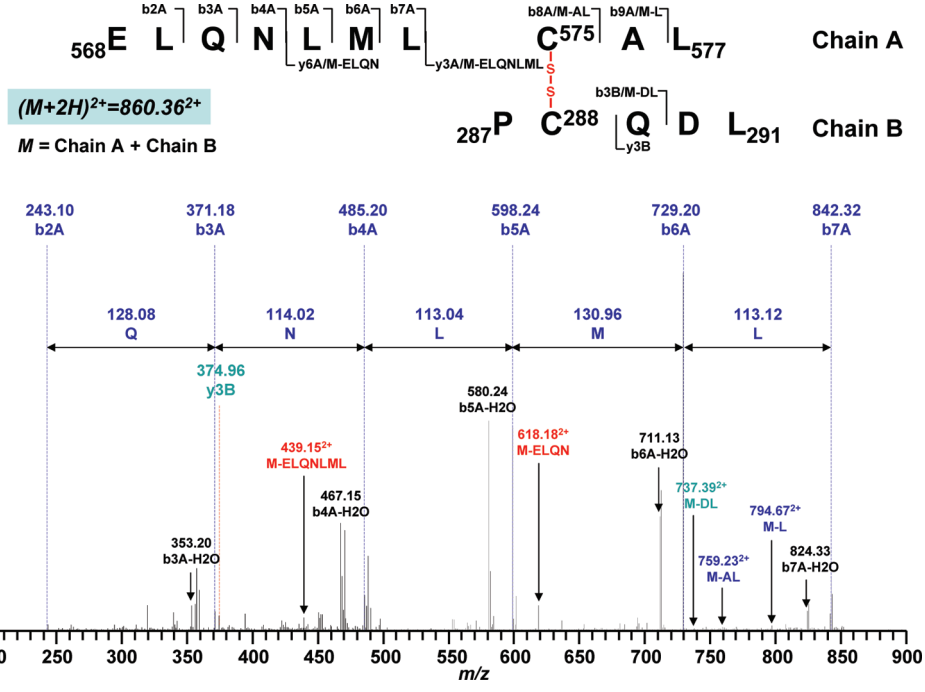

FIGURE 6: Disulfide bond linkage between C_{288} and C_{575} as determined from the MS/MS spectrum of tryptic/chymotryptic digests of the 70 kDa subunit of peroxynitrite-treated complex II. Chain A and chain B represent peptides containing amino acids 568−577 and 287−291, respectively. A disulfide bond linking chain A with chain B is colored red. The sequence-specific ions are labeled as b*n*A (*n* = 2−9) for chain A and y3B and b3B for chain B. M indicates chain A and chain B.

On the basis of the the X-ray structure (Protein Data Bank entry 1ZOY), the C_{306}−C_{312}, C_{439}−C_{444}, and C_{288}−C_{575} distances are 13.4, 11.7, and 6.8 Å, respectively in native complex II. The C_{288}−C_{575} cysteinyl pair is within the reasonable distance [6.4 Å (*16*)] required for disulfide formation. Therefore, it is possible that oxidant stress of complex II by $OONO^-$ induced

Table 2: Detected Fragments Containing Carbamoylmethylated/Alkylated (Addition of -CH_2CONH_2) Cysteines in the 70 kDa Polypeptide of Complex II Treated with Iodoacetamide

theoretical *m*/*z*	detected *m*/*z*	enzyme	fragment	Cys detected
770.4010^{2+}	770.53^{2+}	trypsin	$_{234}$GVIALCIEDGSIHR$_{247}$	C_{239}
513.9364^{3+}	513.84^{3+}	trypsin	$_{234}$GVIALCIEDGSIHR$_{247}$	C_{239}
1122.8617^{3+}	1122.91^{3+}	trypsin	$_{284}$AGLPCQDLEFVQFHPTGIYGAGCLITEGCR $_{313}$	C_{288}, C_{306}, C_{312}
1184.9227^{3+}	1185.58^{3+}	trypsin	$_{556}$GMVWNTDLVETLELQNLMLCALQTIYGAEAR$_{586}$	C_{575}
860.4113^{2+}	860.20^{2+}	chymotrypsin	$_{303}$GAGCLITEGCRGEGGIL$_{319}$	C_{306}, C_{312}
884.4270^{3+}	884.64^{3+}	chymotrypsin	$_{303}$GAGCLITEGCRGEGGILINSQGERF$_{327}$	C_{306}, C_{312}
556.7776^{2+}	556.88^{2+}	chymotrypsin	$_{575}$MICALQTIY$_{581}$	C_{575}
770.4010^{3+}	770.69^{3+}	trypsin and chymotrypsin	$_{234}$GVIALCIEDGSIHR$_{247}$	C_{239}
543.7535^{2+}	543.74^{2+}	trypsin and chymotrypsin	$_{239}$CIEDGSIHR$_{247}$	C_{239}
762.3636^{2+}	762.36^{2+}	trypsin and chymotrypsin	$_{288}$ AGLPCQDLEFVQF$_{296}$	C_{288}
597.2737^{+}	597.34^{+}	trypsin and chymotrypsin	$_{303}$GAGCLITEGCR$_{313}$	C_{306}, C_{312}
860.4113^{2+}	860.46^{2+}	trypsin and chymotrypsin	$_{303}$GAGCLITEGCRGEGGIL$_{319}$	C_{306}, C_{312}
510.8894^{3+}	511.17^{3+}	trypsin and chymotrypsin	$_{438}$ACGEAACASVHGANR$_{452}$	C_{439}, C_{444}
765.8304^{2+}	765.82^{2+}	trypsin and chymotrypsin	$_{438}$ACGEAACASVHGANR$_{452}$	C_{439}, C_{444}
868.4233^{1+}	868.44^{1+}	trypsin and chymotrypsin	$_{575}$CALQTIY$_{581}$	C_{575}

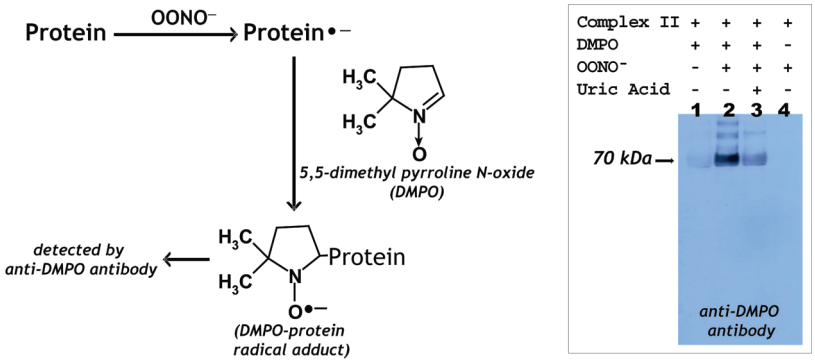

FIGURE 7: Schematic delineation of immuno-spin trapping of the $OONO^-$-induced protein radical with an anti-DMPO polyclonal antibody (left) and detection of the DMPO adduct of the complex II-derived protein radicals by Western blot using an anti-DMPO nitrone adduct polyclonal antibody (right) (lane 2). The reaction mixture contained complex II (treated with dithiothreitol, 1 μM heme *b*) and DMPO (100 mM) in PBS. $OONO^-$ (60 μM) was added to initiate the reaction. The reaction mixture was incubated for 1 h at 37 °C; the reaction was terminated by addition of uric acid (0.2 mM) and sample buffer containing 0.4% SDS and 1% β-ME, and then the mixture was heated at 70 °C for 5 min. Aliquots of 30 pmol of protein were subjected to SDS−PAGE and Western blotting using an anti-DMPO polyclonal antibody. In lane 1, $OONO^-$ was removed from the complete system. In lane 3, uric acid (1.0 mM) was preincubated with complex II and DMPO before the reaction was initiated with $OONO^-$. In lane 4, DMPO was omitted from the complete system.

some conformational changes to facilitate the formation of the $C_{306}-C_{312}$ and $C_{439}-C_{444}$ disulfide pairs. These conformational changes mediated by $OONO^-$ likely impaired the electron transfer activity of complex II, leading to mitochondrial dysfunction.

Peroxynitrite-Mediated Protein Radical Formation in the 70 kDa Subunit of Complex II. It has been reported that $O_2^{\bullet-}$ production by complex II induced self-inactivation through the mechanism in which $O_2^{\bullet-}$ may induce oxidative attack on the protein matrix of complex II, forming the protein radical (*5*). A similar mechanism of protein radical formation resulting from $O_2^{\bullet-}$ attack was observed in the flavoprotein subcomplex of complex I (*17*). $OONO^-$-mediated one-electron oxidation of albumin in human plasma, forming a protein-derived thiyl radical, has been reported and implicated to be a cytotoxic mechanism of $OONO^-$ (*18*). We hypothesize that oxidative modification with protein radical formation can be induced with $OONO^-$ (Figure 7, scheme). Immuno-spin trapping with an anti-DMPO (DMPO, 5,5-dimethylpyrroline *N*-oxide) polyclonal antibody was used to define complex II-derived protein radical formation as described previously (*17*, *19*, *20*). Isolated complex II (1 μM based on heme *b*) was incubated with a nitrone spin trap, DMPO (100 mM), in PBS, and the reaction was initiated by the addition of 60 μM $OONO^-$ at 37 °C. After incubation for 1 h, the aliquots were subjected to SDS−PAGE and Western blotting using an anti-DMPO antibody. The immobilized nitrone adduct of complex II was detected by immunoblotting (Figure 7, right panel, lane 2) in the 70 kDa subunit of complex II, indicating the formation of complex II-derived protein radical(s). The detected Western blot signal was entirely dependent on $OONO^-$ (Figure 7, right panel, lane 1) and DMPO (Figure 7, right panel, lane 4). The detected signal of the DMPO adduct could be inhibited by an $OONO^-$ scavenger, uric acid (1 mM, Figure 7, right panel, lane 3), confirming the formation of the protein radical resulting from oxidative attack by $OONO^-$.

Involvement of C_{288} and C_{655} of the 70 kDa Subunit in the DMPO-Binding Sites Determined by Mass Spectrometry. To further provide direct evidence of the molecular mechanism of the complex II-derived radical induced by $OONO^-$, it is imperative to determine the location of DMPO binding. The DMPO nitrone adduct of complex II was subjected to SDS−PAGE under reducing conditions. The protein band at 70 kDa was cut out and subjected to in-gel digestion with trypsin and chymotrypsin, followed by nano-LC−MS/MS analysis. The resulting mass spectra reveal ions that account for >87% of the amino acid sequence of the 70 kDa polypeptide.

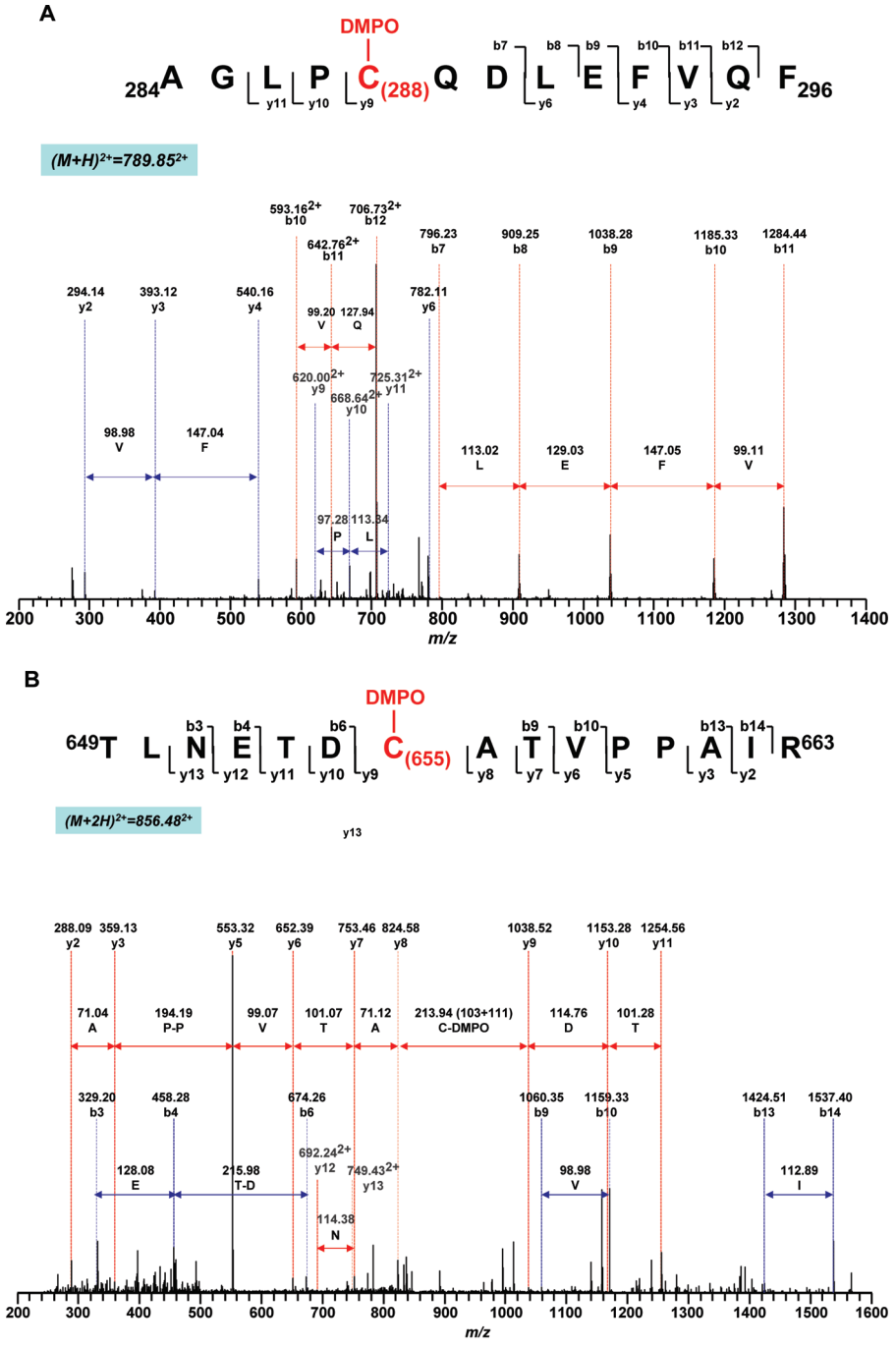

FIGURE 8: MS/MS spectra of the doubly protonated molecular ions of DMPO-binding peptides (A) ^{284}AGLPC^{288}QDLEFVQF^{296} and (B) ^{649}TLNETDC^{655}ATVPPAIR^{663}. The sequence-specific ions are labeled as y and b ions. The amino acid residues involved in DMPO binding are identified as C_{288} and C_{655}.

The binding of DMPO to cysteine residues causes a mass shift of 111 Da to the native intact peptide. Thus, the proteolytic peptides were investigated for the addition of 111 Da to their original intact sequence. This mass difference was observed for one chymotryptic peptide ($_{284}$AGLPC^{288}QDLEFVQF$_{296}$, observed m/z 789.85^{2+} vs theoretical m/z 733.8529^{2+}) and one tryptic peptide ($_{649}$TLNETDC^{655}ATVPPAIR$_{663}$, observed m/z 856.48^{2+} vs theoretical m/z 800.9036^{2+}). Further observation of fragmentation ions y9−y11 and b7−b12 with a mass shift of 111 Da in the tandem mass spectrum of peptide $_{284}$AGLPC^{288}QDLEFVQF$_{296}$ (Figure 8a) suggested that one DMPO molecule is covalently bound to C_{288} in this peptide. Similarly, observation of fragmentation ions y9−y13, b9, b10, b13, and b14 in the MS/MS spectrum of peptide $_{649}$TLNETDC^{655}ATVPPAIR$_{663}$ confirmed that C_{655} was modified by the addition of DMPO (Figure 8b).

C_{288} is located in the large FAD-binding domain, and the residue is surface-exposed (Figure S3B of the Supporting Information). C_{288} (C_{245} in the mature protein) is also involved in formation of the $OONO^-$-mediated disulfide bond with C_{575} (C_{532} in the mature protein) (Figure 6). This distance between C_{288} and C_{575} is 6.8 Å. These results suggest that the protein radical intermediate at C_{288} can participate in the mechanism to facilitate formation of the $OONO^-$-mediated disulfide between C_{288} and C_{575} (eqs 3 and 4). The protein radical at C_{288} likely plays a catalytic role in the formation of the disulfide bond with C_{575}, which may indirectly contribute to $OONO^-$-mediated

complex II impairment.

$$Cys_{288}\text{-}SH \xrightarrow{OONO^-} Cys_{288}\text{-}S^{\bullet} \quad (3)$$

$$Cys_{288}\text{-}S^{\bullet} + Cys_{575}\text{-}SH \rightarrow Cys_{288}\text{-}S\text{-}S\text{-}Cys_{575} \quad (4)$$

C_{655} is located in the C-terminal domain and highly surface-exposed (Figure S3B of the Supporting Information) on the basis of the X-ray structure. It is not likely that protein radical formation at C_{655} significantly affected the moiety of FAD due to a longer distance (24 Å). However, protein thiyl radical is a highly reactive species capable of addition even across carbon−carbon double bonds and possibly capable of initiating lipid peroxidation (*21*, *22*), leading to mitochondrial dysfunction. C_{655} has been identified as the other secondary site (C_{90} is the primary site) involved in S-glutathionylation induced by GSH/GSSG in vitro (*2*). C_{655} is also associated with formation of the protein radical that resulted from oxidative attack of $O_2^{\bullet -}$ (*2*). These data provide evidence of the possible involvement of protein-derived thiyl radical in the reactive glutathionylating species that may contribute to S-glutathionylation at C_{655} in the presence of GSH (eq 5).

$$Cys_{655}\text{-}S^{\bullet} + GSH \rightarrow Cys_{655}\text{-}S\text{-}SG \quad (5)$$

CONCLUSIONS

Mitochondrial thiols are composed of protein thiols and the GSH pool. The proteins of the mitochondrial electron transport chain are rich in protein thiols. Therefore, the protein thiols of ETC appear to play a critical role in controlling the redox state of mitochondria. Mitochondrial complex II is the major component of the ETC and hosts both structural thiols involved in the ligands of iron−sulfur clusters and the reactive or regulatory thiols that are thought to have biological functions, i.e., antioxidant and redox signaling. For example, the physiological role of complex II-derived thiols has been related to inhibition of respiration by nitrosative stress (*23*) and redox modification with S-glutathionylation during myocardial ischemia and reperfusion (*2*).

Despite the fact that the in vivo relevance remains to be investigated, our data obtained from the in vitro model in this study should provide deeper insights into the major mechanism of $OONO^-$-mediated oxidative modification. These studies revealed C_{267}, C_{476}, C_{537}, C_{306}, C_{312}, C_{439}, C_{444}, C_{288}, C_{575}, and C_{655} (of 18 cysteinyl residues available on the 70 kDa subunit) are involved in oxidative modifications by $OONO^-$. C_{288} is likely the primary reactive thiol in response to $OONO^-$ since C_{288} participates in the formation of protein radical and disulfide linkage (Table 1). $OONO^-$-mediated oxidation of C_{537} (S-sulfonation) and C_{655} (protein thiyl radical) is related to the redox event of complex II-derived S-glutathionylation. It has been documented that S-glutathionylation of the complex II 70 kDa subunit preserves enzymatic inactivation by $OONO^-$ (*3*). Therefore, S-glutathionylation of C_{537} and C_{655} should protect the residues from S-sulfonation and protein thiyl radical formation induced by $OONO^-$. In contrast, deglutathionylation under highly reductive conditions (ischemia) facilitates sulfonation and protein radical formation under oxidative conditions (reperfusion) (*2*). Formation of C_{306}−C_{312} and C_{439}−C_{444} disulfides should result from the $OONO^-$-induced conformational change in the 70 kDa protein.

The milieu of the mitochondrial matrix is anoxic in the presence of the GSH/GSSG pool under normal physiological conditions (*24*). Analysis of redox compartmentalization indicates that the relative redox states from most reductive to most oxidative are as follows: mitochondria > nuclei > endoplamic reticulum > extracellular space (*24*). Thus, we expect that a low oxygen tension in the mitochondrial environment should facilitate the free thiol state for most cysteines of the complex II 70 kDa subunit; mitochondrial thiols are the targets of oxidants such as $OONO^-$. They are vulnerable to oxidation such as S-sulfonation, protein-thiyl radical, and disulfide formation. Recognition of this molecular event is valuable in understanding the fundamental basis of disease pathogenesis of myocardial infarction.

ACKNOWLEDGMENT

We thank Dr. Bradley E. Sturgeon (Department of Chemistry, Monmouth University, Monmouth, IL) for critical review of the manuscript.

SUPPORTING INFORMATION AVAILABLE

LC−MS/MS evidence of peroxnitrite-mediated S-sulfonation of C_{476} and C_{537} (Figures S1 and S2) and formation of an intrachain disulfide between C_{439} and C_{444} (Figure S4) and X-ray structure of mammalian complex II (Protein Data Bank entry 1ZOY) showing the surface-exposed nature of specific cysteinyl residues (C_{267}, C_{476}, C_{537}, C_{288}, and C_{655}) susceptible to oxidative modifications by peroxynitrite (Figure S3). This material is available free of charge via the Internet at http://pubs.acs.org.

REFERENCES

1. Lemos, R. S., Fernandes, A. S., Pereira, M. M., Gomes, C. M., and Teixeira, M. (2002) Quinol:fumarate oxidoreductases and succinate: quinone oxidoreductases: Phylogenetic relationships, metal centres and membrane attachment. *Biochim. Biophys. Acta 1553*, 158–170.
2. Chen, Y. R., Chen, C. L., Pfeiffer, D. R., and Zweier, J. L. (2007) Mitochondrial Complex II in the Post-ischemic Heart: Oxidative Injury and the Role of Protein S-Glutathionylation. *J. Biol. Chem. 282*, 32640–32654.
3. Chen, C. L., Chen, J., Rawale, S., Varadharaj, S., Kaumaya, P. P., Zweier, J. L., and Chen, Y. R. (2008) Protein tyrosine nitration of the flavin subunit is associated with oxidative modification of mitochondrial complex II in the post-ischemic myocardium. *J. Biol. Chem. 283*, 27991–28003.
4. Liu, B., Tewari, A. K., Zhang, L., Green-Church, K. B., Zweier, J. L., Chen, Y. R., and He, G. (2009) Proteomic analysis of protein tyrosine nitration after ischemia reperfusion injury: Mitochondria as the major target. *Biochim. Biophys. Acta 1794*, 476–485.
5. Zhao, X., Chen, Y. R., He, G., Zhang, A., Druhan, L. J., Strauch, A. R., and Zweier, J. L. (2007) Endothelial nitric oxide synthase (NOS_3) knockout decreases NOS_2 induction, limiting hyperoxygenation and conferring protection in the postischemic heart. *Am. J. Physiol. 292*, H1541–H1550.
6. Zhao, X., He, G., Chen, Y. R., Pandian, R. P., Kuppusamy, P., and Zweier, J. L. (2005) Endothelium-derived nitric oxide regulates post-ischemic myocardial oxygenation and oxygen consumption by modulation of mitochondrial electron transport. *Circulation 111*, 2966–2972.
7. Wang, P., and Zweier, J. L. (1996) Measurement of nitric oxide and peroxynitrite generation in the postischemic heart. Evidence for peroxynitrite-mediated reperfusion injury. *J. Biol. Chem. 271*, 29223–29230.
8. Garg, V., and Hu, K. (2007) Protein kinase C isoform-dependent modulation of ATP-sensitive K^+ channels in mitochondrial inner membrane. *Am. J. Physiol. 293*, H322–H332.
9. Lee, G. Y., He, D. Y., Yu, L., and Yu, C. A. (1995) Identification of the ubiquinone-binding domain in QPs1 of succinate-ubiquinone reductase. *J. Biol. Chem. 270*, 6193–6198.
10. Yu, L., and Yu, C. A. (1982) Quantitative resolution of succinate-cytochrome c reductase into succinate-ubiquinone and ubiquinol-cytochrome c reductases. *J. Biol. Chem. 257*, 2016–2021.

11. Hatefi, Y. (1978) Preparation and properties of succinate:ubiquinone oxidoreductase (complex II). *Methods Enzymol. 53*, 21–27.
12. Zhang, L., Xu, H., Chen, C. L., Green-Church, K. B., Freitas, M. A., and Chen, Y. R. (2008) Mass spectrometry profiles superoxide-induced intramolecular disulfide in the FMN-binding subunit of mitochondrial Complex I. *J. Am. Soc. Mass Spectrom. 19*, 1875–1886.
13. Xu, H., and Freitas, M. A. (2007) A mass accuracy sensitive probability based scoring algorithm for database searching of tandem mass spectrometry data. *BMC Bioinf. 8*, 133.
14. Han, Z., Chen, Y. R., Jones, C. I., III, Meenakshisundaram, G., Zweier, J. L., and Alevriadou, B. R. (2007) Shear-induced reactive nitrogen species inhibit mitochondrial respiratory complex activities in cultured vascular endothelial cells. *Am. J. Physiol. 292*, C1103–C1112.
15. Sun, F., Huo, X., Zhai, Y., Wang, A., Xu, J., Su, D., Bartlam, M., and Rao, Z. (2005) Crystal structure of mitochondrial respiratory membrane protein complex II. *Cell 121*, 1043–1057.
16. Seeger, M. A., von Ballmoos, C., Eicher, T., Brandstatter, L., Verrey, F., Diederichs, K., and Pos, K. M. (2008) Engineered disulfide bonds support the functional rotation mechanism of multidrug efflux pump AcrB. *Nat. Struct. Mol. Biol. 15*, 199–205.
17. Chen, Y. R., Chen, C. L., Zhang, L., Green-Church, K. B., and Zweier, J. L. (2005) Superoxide generation from mitochondrial NADH dehydrogenase induces self-inactivation with specific protein radical formation. *J. Biol. Chem. 280*, 37339–37348.
18. Vasquez-Vivar, J., Santos, A. M., Junqueira, V. B., and Augusto, O. (1996) Peroxynitrite-mediated formation of free radicals in human plasma: EPR detection of ascorbyl, albumin-thiyl and uric acid-derived free radicals. *Biochem. J. 314*, 869–876.
19. Detweiler, C. D., Deterding, L. J., Tomer, K. B., Chignell, C. F., Germolec, D., and Mason, R. P. (2002) Immunological identification of the heart myoglobin radical formed by hydrogen peroxide. *Free Radical Biol. Med. 33*, 364–369.
20. Chen, Y. R., Chen, C. L., Liu, X., Li, H., Zweier, J. L., and Mason, R. P. (2004) Involvement of protein radical, protein aggregation, and effects on NO metabolism in the hypochlorite-mediated oxidation of mitochondrial cytochrome c. *Free Radical Biol. Med. 37*, 1591–1603.
21. Schoneich, C., Asmus, K. D., Dillinger, U., and von Bruchhausen, F. (1989) Thiyl radical attack on polyunsaturated fatty acids: A possible route to lipid peroxidation. *Biochem. Biophys. Res. Commun. 161*, 113–120.
22. Schoneich, C., Dillinger, U., von Bruchhausen, F., and Asmus, K. D. (1992) Oxidation of polyunsaturated fatty acids and lipids through thiyl and sulfonyl radicals: Reaction kinetics, and influence of oxygen and structure of thiyl radicals. *Arch. Biochem. Biophys. 292*, 456–467.
23. Shiva, S., Crawford, J. H., Ramachandran, A., Ceaser, E. K., Hillson, T., Brookes, P. S., Patel, R. P., and Darley-Usmar, V. M. (2004) Mechanisms of the interaction of nitroxyl with mitochondria. *Biochem. J. 379*, 359–366.
24. Hansen, J. M., Go, Y. M., and Jones, D. P. (2006) Nuclear and mitochondrial compartmentation of oxidative stress and redox signaling. *Annu. Rev. Pharmacol. Toxicol. 46*, 215–234.